JOURNAL OF GEOPHYSICAL RESEARCH, VOL. 101, NO. D18, PAGES 23,299–23,309, OCTOBER 27, 1996

Absorption of solar radiation by clouds: Interpretations of satellite, surface, and aircraft measurements

R. D. Cess, M. H. Zhang, Y. Zhou, X. Jing, and V. Dvortsov

Marine Sciences Research Center, Institute for Terrestrial and Planetary Atmospheres, State University of New York, Stony Brook

Abstract. To investigate the absorption of shortwave radiation by clouds, we have collocated satellite and surface measurements of shortwave radiation at several locations. Considerable effort has been directed toward understanding and minimizing sampling errors caused by the satellite measurements being instantaneous and over a grid that is much larger than the field of view of an upward facing surface pyranometer. The collocated data indicate that clouds absorb considerably more shortwave radiation than is predicted by theoretical models. This is consistent with the finding from both satellite and aircraft measurements that observed clouds are darker than model clouds. In the limit of thick clouds, observed top-of-the-atmosphere albedos do not exceed a value of 0.7, whereas in models the maximum albedo can be 0.8.

1. Introduction

Since the early suggestion by *Fritz* [1951] that clouds absorb about 3 times more shortwave (SW) radiation than predicted by theoretical models, there has been considerable confusion as to how much SW radiation clouds actually do absorb. Comprehensive summaries of this issue are given by *Stephens and Tsay* [1990] and by *Liou* [1992]. It is important to note that the aircraft observations they discuss refer to radiometric measurements of isolated clouds. In an aircraft experiment performed by *King et al.* [1990] the cloud single-scattering albedo was determined from measurements made within a marine stratocumulus cloud. Their findings show little evidence of enhanced cloud SW absorption, implying that if such absorption does exist, it would be of a macrophysical rather than microphysical nature. This, in fact, is the argument used by *Stephens and Greenwald* [1991] to explain their conclusion, which was based on satellite radiometric data, that observed clouds are significantly darker than model clouds. Darker clouds do not, however, necessarily mean that clouds absorb more SW radiation; they might instead be darker because more downward SW radiation is transmitted through them. However, several studies suggest the reverse, that models overestimate the SW radiation absorbed at the surface, which means they are overestimating surface insolation and thus overestimating atmospheric transmittance. Thus darker clouds that simultaneously reduce the column transmittance of the atmosphere have only one explanation, they increase the SW absorption by the atmospheric column.

Wild et al. [1995] have compared several general circulation models (GCMs) to the global energy balance archive (GEBA) data for SW radiation absorbed at the surface. The GCMs produced a global-mean range from 162 to 185 W m^{-2}, compared to 142 W m^{-2} derived from the GEBA data. In that most GCMs are "tuned" to satellite radiometric data at the top of the atmosphere (TOA), the GCM versus GEBA differences in surface SW absorption suggest the GCMs are underestimating atmospheric SW absorption by 20–43 W m^{-2}. To place these numbers in perspective, *Kiehl et al.* [1995] increased global-mean atmospheric absorption through increasing cloud absorption by 22 W m^{-2} in version 2 of the National Center for Atmospheric Research (NCAR) Community Climate Model (CCM2). The impact of this on the behavior of the model was dramatic. The upper troposphere warmed by as much as 4 K, and the strength of the Hadley circulation was reduced by 12%, which lead to lower surface wind speeds that in turn reduced the surface latent heat flux by 25 W m^{-2}.

A recent modeling study, performed as part of the Clouds and the Earth's Radiant Energy System/Atmospheric Radiation Measurements/Global Energy and Water Cycle Experiment (CAGEX) by T. Alberta and T. Charlock (private communication, 1996; this information is available from the CAGEX home page, World Wide Web, http://snowdog.larc-.nasa.gov:/cagex.html), directly addresses the issue of cloud impacts on atmospheric transmittance. They used surface insolation measurements during April 5–30, 1994, obtained as part of the Atmospheric Radiation Measurements (ARM) program in Oklahoma, which provided direct observations of atmospheric transmittance. They also implemented observations of cloud amount, cloud liquid water content, column water vapor, aerosol optical depth, and surface albedo into the atmospheric radiative transfer code developed by *Fu and Liou* [1993], which thus provided model transmittances as determined from the Fu-Liou code. The Alberta and Charlock model versus observed atmospheric transmittances are summarized in Figure 1 and raise two issues. First, the model overestimates clear-sky transmittances by an average of 5%, and further discussion of this is given later in this section. However, the second and more important issue is that when clouds are present (all sky) the model overestimate is much larger (11%), indicating the model clouds result in an overestimate of atmospheric transmittance. Thus the collective conclusion of the studies by *Stephens and Greenwald* [1991], *Wild et al.* [1995], and T. Alberta and T. Charlock (private communication, 1996) is that relative to model clouds real clouds produce greater absorption of SW radiation within the atmospheric column.

There are suggestions that this phenomenon, at least in part,

Paper number 96JD02156.
0148-0227/96/96JD-02156$09.00

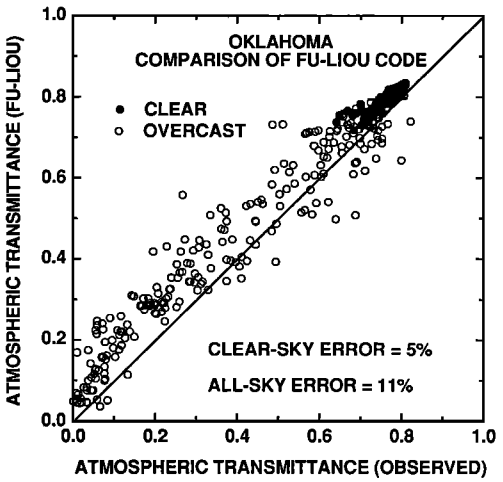

Figure 1. Comparison of atmospheric transmittance evaluated from the Fu-Liou code by T. Alberta and T. Charlock (private communication, 1996) (see text) to that observed at the Atmospheric Radiation Measurements (ARM) Oklahoma site during April 1994.

is of a macrophysical rather than microphysical nature. As previously discussed, cloud single-scattering albedos determined by *King et al.* [1990] show little evidence of enhanced cloud SW absorption, which tends to rule out uncertainties in this aspect of cloud microphysics. Moreover, employing a plane-parallel cloud model, *Chou et al.* [1995] conclude that there would have to be substantial revisions to our understanding of cloud microphysics in order for a plane-parallel model to produce significant cloud SW absorption. On the other hand, a modeling study by *Byrne et al.* [1996] concluded that cloud morphology produced enhanced cloud absorption in their model. Also, a three-dimensional Monte-Carlo simulation by W. O'Hirok and C. Gautier, private communication, 1996) produced enhanced cloud absorption relative to a plane-parallel model. An observational study by *Loeb and Davies* [1996, p. 1621] noted that "three-dimensional cloud structures not accounted for by plane parallel theory have a statistically important effect on the radiation field," which again emphasizes the importance of cloud morphology.

A new and innovative approach to addressing the measurement of cloud SW absorption was put forth by *Ramanathan et al.* [1995] using Central Equatorial Pacific Experiment (CEPEX) data for the western Pacific warm pool. They adopted the concept of cloud-radiative forcing (CRF), which refers to the difference between all-sky (cloudy sky) and clear-sky net downward (downward minus upward) SW radiation, either at the TOA or at the surface. Thus CRF delineates the radiative impact of clouds. The warm pool results of *Ramanathan et al.* [1995] are schematically illustrated in Figure 2. The CRF = -65 W m^{-2} at the TOA means that clouds cool, through reflection of SW radiation, the surface-atmosphere system by 65 W m^{-2}. Theoretical radiative transfer models typically predict that cloudy skies absorb about the same amount of SW radiation as do clear skies, as will be demonstrated later in this section, which means that CRF at the surface should be the same as at the TOA [*Ramanathan et al.*, 1995]. However, Ramanathan et al. found that CRF = -100 W m^{-2} at the surface, a discrepancy that can only be explained by the cloudy sky absorbing 35 W m^{-2} more SW radiation than the clear sky for the warm pool region. It is important to note that unlike most aircraft experiments this approach does not focus on a single isolated cloud. Instead, the results summarized in Figure 2 represent a long-term temporal average of cloud systems. Because of sampling issues, Ramanathan et al. determined the surface CRF as the residual of the other components of the surface energy budget, rather from a direct measurement. Recently, however, *Waliser et al.* [1996] have obtained this directly from buoy measurements. Their value for CRF at the surface, -103 W m^{-2}, is nearly identical to that of *Ramanathan et al.* [1995] (Figure 2).

At the same time, yet another novel measurement program was being performed, again in the tropical western Pacific. *Pilewskie and Valero* [1995] flew two stacked aircraft at fixed altitudes and measured atmospheric absorption between the aircraft altitudes. Like *Ramanathan et al.* [1995], they observed cloud systems and found the same CRF discrepancies, and thus the same enhanced cloud SW absorption. As *Pilewskie and Valero* [1996] have recently emphasized, their focus on spatial averaging of cloud systems eliminated a sampling error associated with measurements of an isolated cloud [*Ackerman and Cox*, 1981].

Simultaneous with the above, *Cess et al.* [1995] addressed the cloud SW absorption issue by collocating satellite and surface SW measurements at five geographically diverse locations. Like *Ramanathan et al.* [1995] and *Pilewskie and Valero* [1995], they also observed cloud systems and also found substantial enhanced cloud SW absorption. Their results for GOES satellite measurements that were collocated with near-surface measurements made at the Boulder Atmospheric Observatory (BAO) tower are summarized in Figure 3a using the same format as in Figure 2 for the warm pool. A detailed description of this data is provided in the next section. Like the warm pool, the surface CRF is larger in magnitude than that at the TOA but by a slightly smaller ratio (1.4 compared to 1.5 for the warm pool). The primary cause of the difference in excess cloudy-sky SW absorption relative to clear skies (16 W m^{-2} compared to 35 W m^{-2} for the warm pool), however, is because there are more clouds present at the warm pool and more cloud absorption, as evidenced by the much greater CRF values, both at the surface and at the TOA, for the warm pool relative to Boulder. Differences in the TOA insolation between the two sites also cause differences in CRF, but this is a small effect because the BAO tower data are for the summer when the TOA insolation is large and comparable to that at the warm pool.

As previously discussed, theoretical radiative transfer models typically predict that cloudy skies absorb about the same

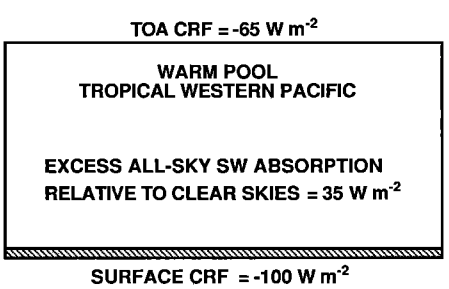

Figure 2. Schematic illustration of the CEPEX results of *Ramanathan et al.* [1995] for the tropical western Pacific warm pool.

amount of SW radiation as do clear skies so that the excess all-sky absorption, relative to clear skies, in Figures 2 and 3a represents the difference in all-sky absorption relative to models as caused by excess cloud SW absorption. The Boulder data serve to demonstrate this point. Compared in Figure 3b is the atmospheric absorptance (fraction of the TOA insolation absorbed by the atmosphere), as evaluated from the BAO tower collocated data and from output from CCM2 for a grid representative of Boulder and for the same time period. For CCM2, it will be shown that the CRF at the surface is virtually the same as that at the TOA, consistent with typical radiative transfer models, and from prior discussion this in turn means that the clear-sky and overcast-sky atmospheric SW absorption is essentially the same, as is consistent with the CCM2 results shown in Figure 3b. The observations at the BAO tower likewise show consistency in the two interpretations. That the magnitude of CRF at the surface is greater than at the TOA (Figure 3a) means that overcast skies absorb more SW radiation than do clear skies, as is clearly demonstrated in Figure 3b. For clear skies, CCM2 is in excellent agreement with the observed absorptance, whereas for overcast skies the observed absorptance is nearly 30% greater than CCM2 and for the clear-sky observations. The clear-sky agreement is in contrast to the clear-sky model and observational differences (5%) shown in Figure 1 for Oklahoma, and there is recent evidence that the latter may be an artifact of an instrumental bias. However, a 5% instrument bias would still result in a substantial (6%) all-sky error in Figure 1.

The purpose of the present study is to extend and clarify certain aspects of the *Cess et al.* [1995] investigation. To a limited extent, aircraft measurements will be employed to supplement conclusions resulting from satellite measurements. Because clouds are three dimensional, sampling errors can occur when collocating satellite and surface measurements, and an examination of sampling issues is provided in section 2. Following section 2 is a comparison and interpretation of the measurements with models.

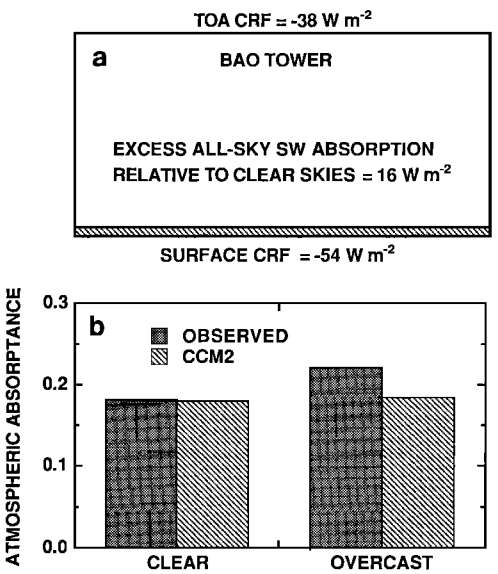

Figure 3. (a) Schematic illustration of the results of *Cess et al.* [1995] for the Boulder Atmospheric Observatory (BAO) tower. (b) Comparison of atmospheric absorptance as determined from CCM2 to that observed at the BAO tower, for both clear and overcast conditions.

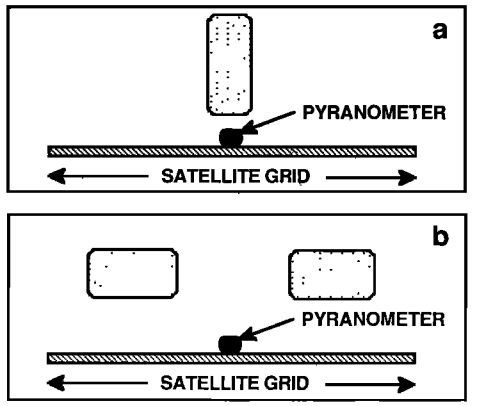

Figure 4. Schematic illustration of satellite surface sampling errors caused by broken clouds. (a) A single isolated cloud that impacts the surface measurement while having little effect on the satellite measurement and (b) same as Figure 4a, except for clouds over most of the satellite grid but not over the surface.

2. Sampling Issues

2.1. Spatial and Temporal Sampling Errors

A significant contributor to measurement errors associated with collocated satellite-surface measurements are sampling errors, which occur because the satellite pixel measurements are instantaneous and over a grid that is much larger than the field of view of an upward facing pyranometer. As schematically illustrated in Figure 4a, a single isolated cloud could substantially impact the surface measurement while having little effect on the satellite measurement; the reverse would occur if there were clouds over most of the satellite grid but not over the surface instrument (Figure 4b). Cloud systems move, however, so that, in a statistical context, temporally averaging the surface measurements can be equivalent to spatially averaging them over the satellite grid. This equivalence between temporal and spatial averaging is conveniently demonstrated by using the collocated GOES-pyranometer measurements of *Cess et al.* [1995] for a region in Wisconsin. The surface measurements are from a network of 11 pyranometers located within a roughly 0.8° × 0.8° grid for the period October 12, 1986, to November 2, 1986, and they are available as 1-min means. The TOA measurements consist of broadband (0.2–5.0 μm) albedos computed from visible channel (0.55–0.70 μm) GOES brightness counts [*Minnis et al.*, 1992, 1993] for 8 × 8 arrays of hourly GOES-East 1-km pixels over each of the 11 pyranometer locations.

A scatterplot of TOA albedo versus atmospheric transmittance (surface insolation divided by TOA insolation) is shown in Figure 5 for which the data have been averaged over all of the 11 surface stations. This constitutes the ideal case of spatial averaging; the temporal averaging period is 1 min. The linear dependence is emphasized by the fact that a quadratic fit cannot be distinguished from the linear fit. To demonstrate the equivalence of temporal and spatial averaging, a single station (Reedsburg) has been chosen. The albedo α versus transmittance T slope, $\Delta\alpha/\Delta T$, is shown in Figure 6 as a function of the Reedsburg surface averaging period (temporally centered about the time of the satellite measurement) and compared to $\Delta\alpha/\Delta T = -0.637$ from the all-station spatial average with 1-min surface averaging (Figure 5). Close agreement is obtained for a Reedsburg surface averaging period of roughly 60

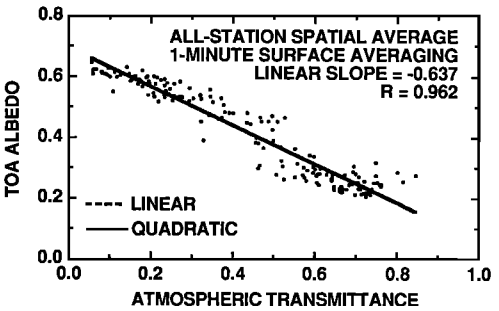

Figure 5. The top-of-the-atmosphere (TOA) albedo versus atmospheric transmittance scatterplot for Wisconsin. The data have been spatially averaged over the 11 surface stations, and the surface averaging period is 1 min.

min. The same conclusion can be reached independently of the other instruments; the optimum surface averaging period corresponds to the maximum correlation coefficient (Figure 6).

To better understand the nature of temporal and spatial sampling errors, a schematic demonstration is given in Figure 7a of the two types of sampling errors illustrated in Figures 4a and 4b. For Figure 4a, the cloud has a lesser impact on the TOA albedo, as measured over the satellite grid, than on the surface pyranometer with its smaller field of view. Thus, relative to the pyranometer-derived transmittance, this type of sampling error produces an underestimate of the TOA albedo (Figure 7a). The reverse occurs for sampling errors of the type illustrated in Figure 4b and schematically shown in Figure 7a. In addition, if the clouds depicted in Figure 4b supplied diffuse radiation to the surface pyranometer, this would amplify the sampling error by increasing the measured surface insolation and thus increasing the transmittance. It is important to note that when evaluating $\Delta\alpha/\Delta T$, such errors are not compensatory upon averaging; they instead act to systematically reduce the magnitude of $\Delta\alpha/\Delta T$ as demonstrated in Figure 7a. This is because errors of the type shown in Figure 4a reduce the TOA albedo when the pyranometer-derived transmittance is intermediate or small (because of the overlying cloud). In contrast,

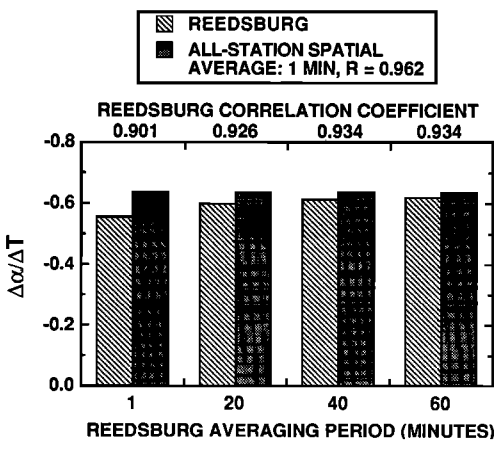

Figure 6. The albedo α versus transmittance T ($\Delta\alpha/\Delta T$) for a single station (Reedsburg) of the Wisconsin pyranometer network as a function of the surface averaging period at that site, and as determined by spatially averaging the 11 stations within the network. The all-station spatial average adopts 1-min surface averaging and invariant to the Reedsburg averaging period.

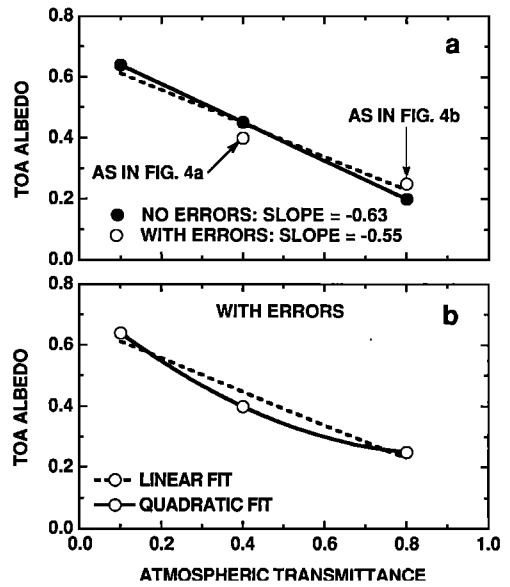

Figure 7. Schematic illustration of the impact of the sampling errors illustrated in Figure 4 on the relationship of the TOA albedo to the atmospheric transmittance.

errors of the type shown in Figure 4b increase the TOA albedo when the pyranometer-derived transmittance is large. As demonstrated by *Cess et al.* [1995] and as further discussed in the following section, $\Delta\alpha/\Delta T$ serves as one measure of cloud absorption, with increased cloud absorption corresponding to a reduction in the magnitude of $\Delta\alpha/\Delta T$. Thus it is important to realize that when interpreting cloud absorption in terms of $\Delta\alpha/\Delta T$, sampling errors could lead to an overestimate of cloud absorption.

Sampling errors should also manifest themselves by producing a departure from linearity, as indicated by the quadratic departure from linearity shown in Figure 7b. The data for Reedsburg serve to demonstrate this point. For 1-min surface averaging, there is a quadratic departure from linearity (Figure 8a), which is not the case for 60-min surface averaging (Figure 8b). Recall that the surface averaging period refers to temporally centered GOES measurements that are made hourly. Thus the number of collocated data is invariant to the duration of the surface averaging period. The similarity of Figure 8b (temporal averaging) to Figure 5 (spatial averaging) again emphasizes the equivalence of spatial and temporal averaging.

This spatial-temporal equivalence has been demonstrated in a somewhat different manner by *Long and Ackerman* [1995], who also used the Wisconsin data. They showed that for any pair of pyranometers the correlation coefficient between temporal averages at the two locations increased monotonically with averaging period. Long and Ackerman further showed that the standard deviation computed for pairs of pyranometers was almost a unique function of the correlation coefficient for the two locations, regardless of the location separation or averaging period. Thus this is an implicit demonstration of the equivalence of spatial and temporal sampling.

2.2. Related Sampling Issues

A discussion of related sampling issues begins with a reanalysis of the Boulder-GOES data used by *Cess et al.* [1995]. These consist of TOA broadband albedos computed from GOES brightness counts averaged over 12 × 12 arrays of

half-hourly GOES-West 1-km pixels [*Minnis et al.*, 1992]. Hourly means were then computed from three consecutive half-hourly GOES measurements and temporally collocated with hourly mean pyranometer measurements made at the top of the 300-m Boulder Atmospheric Observatory tower for the period June 29, 1987, to July 19, 1987. Both upward and downward facing pyranometers were situated on the tower, thus providing near-surface measurements of both net downward SW radiation and insolation.

Because cloud-radiative forcing refers to the difference between all-sky (cloudy sky) and clear-sky net downward (downward minus upward) SW radiation either at the TOA or at the surface, its evaluation requires the identification of clear-sky measurements. The GOES clear-sky identification was used at the TOA, and a linear fit to these measurements is shown in Figure 9a. The difference between each measurement and the clear-sky fit thus provides values of CRF(TOA) for each measurement, producing a dayside mean of -63 W m^{-2} (Figure 9a), from which the diurnal mean shown in Figure 3a (-38 W m^{-2}) was obtained. The hourly-mean surface measurements were identified as clear if GOES identified the entire satellite grid as clear for the three consecutive half-hourly measurements that coincided with the hourly-mean surface measurements. This produced a dayside-mean surface (SRF)CRF of CRF(SRF) = -88 W m^{-2} (Figure 9b), a factor of 1.4 greater than CRF(TOA). Although the CRF(SRF)/CRF(TOA) ratio was adopted in previous studies [*Ramanathan et al.*, 1995; *Cess et al.*, 1995; *Ptlewskie and Valero*, 1995], for present purposes, it will be more convenient to employ the reciprocal ratio, CRF(TOA)/CRF(SRF) = 0.716.

At other locations, measurements of only surface insolation were available, and so it was not possible to evaluate CRF (SRF). However, a comparable forcing, defined in terms of surface insolation, cloud-insolation forcing (CIF)(SRF), rather than surface SW absorption, can be obtained as demonstrated in Figure 9c. Both CRF(TOA)/CRF(SRF) and CRF(TOA)/CIF(SRF) require only that measurement (sampling) errors be random so they average to zero when evaluating the numerator

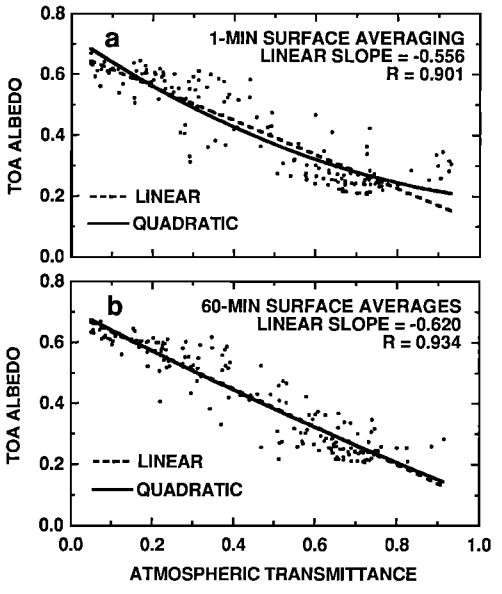

Figure 8. TOA albedo versus atmospheric transmittance scatterplot for Reedsburg showing the surface averaging period for (a) 1 min and (b) 60 min.

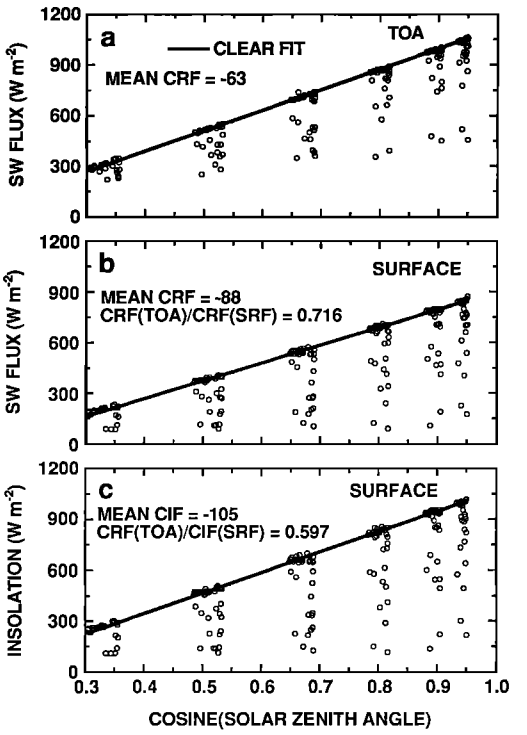

Figure 9. (a) The net downward SW flux at the TOA as measured by GOES at the BAO tower, as a function of the cosine of the solar zenith angle. (b) The same as Figure 9a, but for the tower-measured net SW flux at the surface. (c) The same as Figure 9a, but for the tower-measured insolation at the surface.

and denominator of the ratios. An alternate procedure is to evaluate CRF(TOA)/CIF(SRF) as the linear slope of a CRF(TOA) versus CIF(SRF) regression, as demonstrated in Figure 10a. That the two approaches produce nearly identical results addresses another sampling issue, because the ratio determined from Figures 9a and 9c (0.597) requires only that such errors be random, while the slope in Figure 10a implicitly requires they be in the TOA measurements. If the errors were in the surface measurements, a CIF(SRF) versus CRF(TOA) regression would be required, and the CRF(TOA) versus CIF(SRF) slope would be increased by the factor $1/R^2$, where R is the correlation coefficient, to 0.715, inconsistent with Figure 9c. This clearly demonstrates that sampling errors are associated with the TOA measurements, in part because the TOA hourly means were evaluated from three consecutive half-hourly instantaneous measurements, in contrast to the surface measurements which are true hourly means. This also suggests the hourly-mean surface data, which were the only data available at the BAO tower, are representative of the optimal surface averaging period, consistent with our prior analysis of the Wisconsin data.

One source of uncertainty in Figure 9c and to a lesser extent in Figure 10a, is the validity of the clear-sky identification, both at the TOA and at the surface. The α versus T regression can be used to address this issue. It is straightforward to show that

$$\Delta\alpha/\Delta T = -\mathrm{CRF(TOA)/CIF(SRF)} \qquad (1)$$

The fact that the α versus T regression (Figure 10b) yields, by means of (1), virtually the same CRF(TOA)/CIF(SRF) ratio as in Figure 9c demonstrates the validity of the clear-sky identi-

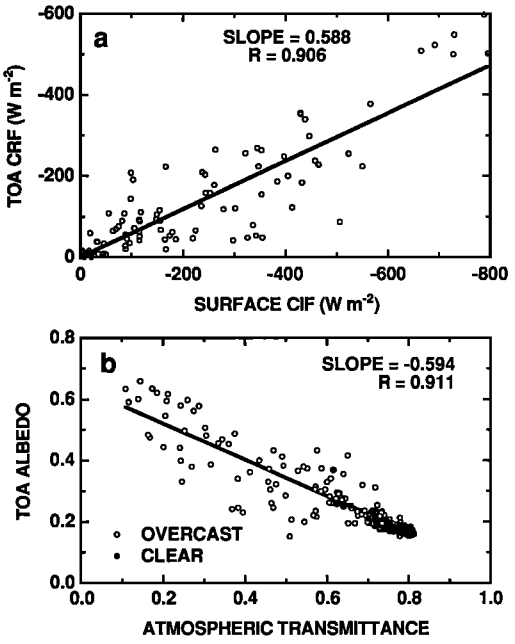

Figure 10. (a) The TOA cloud-radiative forcing (CRF) as a function of the surface cloud-insolation forcing for Boulder. (b) The TOA albedo as a function of atmospheric transmittance for Boulder.

fication, because the slope shown in Figure 10b does not require the identification of clear-sky measurements. In fact, the slope is nearly invariant as to whether the clear data are or are not included; it is −0.594 with the clear data included and −0.587 with the clear data deleted.

3. Comparison With Models

As discussed in the Introduction, T. Alberta and T. Charlock (private communication, 1996) have implemented observed quantities into the radiation code of *Fu and Liou* [1993] for the April 5–30, 1994, ARM Oklahoma experiment. An α versus T scatterplot using these results is shown in Figure 11a together with output for the same time period and for a grid representing Oklahoma from version 2 of the NCAR Community Climate Model (CCM2). Note that the Fu-Liou code produces both larger TOA albedos and smaller transmittances than does CCM2. This is because the former adopts observed cloud liquid water, while the latter produces its own surrogate for cloud liquid water, namely cloud optical depth, and CCM2 is evidently underestimating this quantity. Both models exhibit strong α-T linearity as demonstrated by the linear correlation coefficients shown in Figure 11b. Moreover, the agreement between the models, in terms of slope, indicates the CCM2 radiation code is representative of other cloud radiation models, and thus it is adopted in the following comparisons.

The quantities CRF(TOA)/CRF(SRF), CRF(TOA)/CIF(SRF), and $\Delta\alpha/\Delta T$ all constitute measures of all-sky versus clear-sky SW absorption, and these are compared to CCM2 in Figure 12a. However, within the context of our interpretations of Figures 2 and 3a, it is more convenient to address the reciprocal quantities as compared in Figure 12b. For the same CRF(TOA), CCM2 underestimates the magnitude of CRF(SRF) by 24% because it overestimates the cloudy-sky surface SW absorption by underestimating cloud SW absorption. Thus CCM2 is underestimating surface insolation, as is consistent with the same percentage overestimate in CIF(SRF) as determined from the CRF(TOA)/CIF(SRF) comparison. The $\Delta\alpha/\Delta T$ comparison makes the same point by means of (1).

The above are also consistent with the interpretation of the effect of clouds upon the fractional absorptance of the atmospheric column, as was demonstrated in Figure 3b. For clear skies, CCM2 is in excellent agreement with the observed absorptance, whereas for overcast skies the observed fractional absorptance is nearly 30% greater than that of CCM2 and of that for the clear-sky observations. The point, as emphasized in the Introduction, is that the atmospheric absorption for the model is essentially the same with or without clouds, whereas the observations demonstrate that clouds substantially increase atmospheric absorption.

We next address the issue of real clouds being darker than model clouds as suggested by *Stephens and Greenwald* [1991]. Figure 13a makes this point very clearly. Here the linear fit to the α-T scatterplot for Wisconsin (Figure 5) is compared to that produced by the CCM2 radiation code. For the same atmospheric transmittance, the CCM2 radiation code overestimates the observed TOA albedo except for large transmittance values (clear skies). As the transmittance approaches zero (asymptotic limit of thick clouds), the data show a maximum TOA albedo of about 0.7, while for the CCM2 code it is about 0.8, which is also the case for the Fu-Liou code (Figure 11b) as applied to the Oklahoma data. This difference persists at other locations as demonstrated in Figure 13b, which shows maximum albedos (for $T \rightarrow 0$) as determined for Wisconsin, and from collocated data for American Samoa and Cape Grim [*Cess et al.*, 1995], and as evaluated from CCM2. For present purposes, the 3-year (1985–1987) American Samoa data were extended to 5 years (1985–1989), and a data processing error that affected the original data for December 1986 and throughout 1987 was corrected. Three procedures were used to determine the $T \rightarrow 0$ TOA albedos from both the observations and

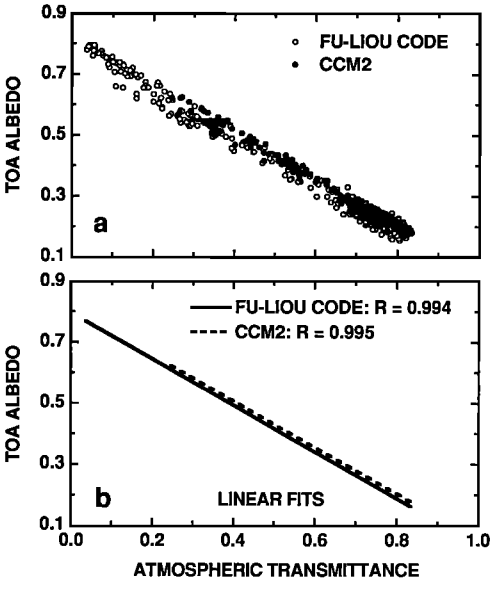

Figure 11. (a) TOA albedo versus atmospheric transmittance scatterplot for the Fu-Liou code and Community Climate Model (CCM2), as representative of the ARM Oklahoma data for April 1994. (b) Same as Figure 11a, but showing only the linear fits.

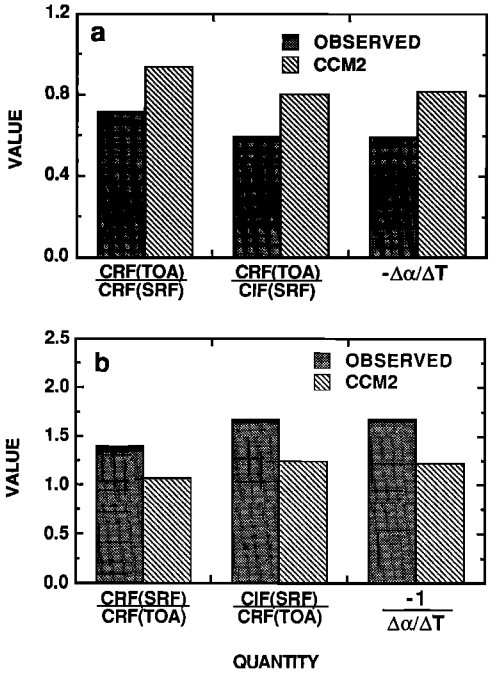

Figure 12. (a) Comparison of observed and CCM2 values of CRF(TOA)/CRF(SRF), CRF(TOA/CIF(SRF), and $\Delta\alpha/\Delta T$ for the BAO tower. (b) The same as Figure 12a but for the reciprocal quantities.

CCM2; linear, quadratic, and cubic extrapolations to $T = 0$. For the observations, we chose the procedure that gave the largest albedo, while for CCM2 it was the procedure that produced the smallest albedo. Thus, even though we have tried to minimize the observational versus model differences in the maximum TOA albedo, they remain substantial (Figure 13b).

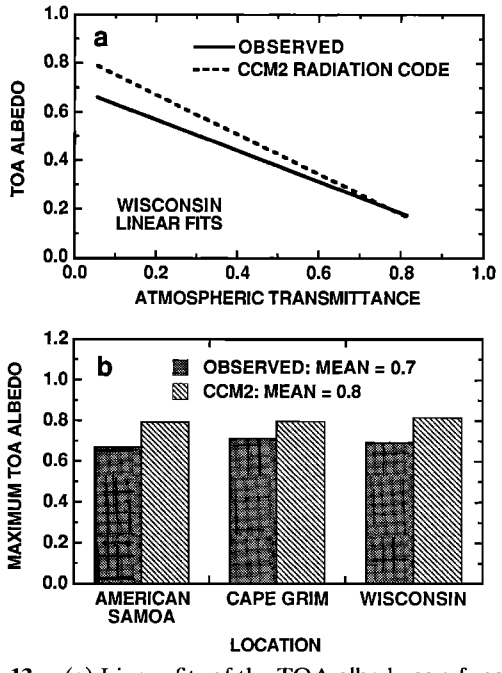

Figure 13. (a) Linear fits of the TOA albedo as a function of atmospheric transmittance for the Wisconsin data and for CCM2. (b) The maximum TOA albedo, for three locations, as determined by extrapolating α versus T scatterplots to $T = 0$.

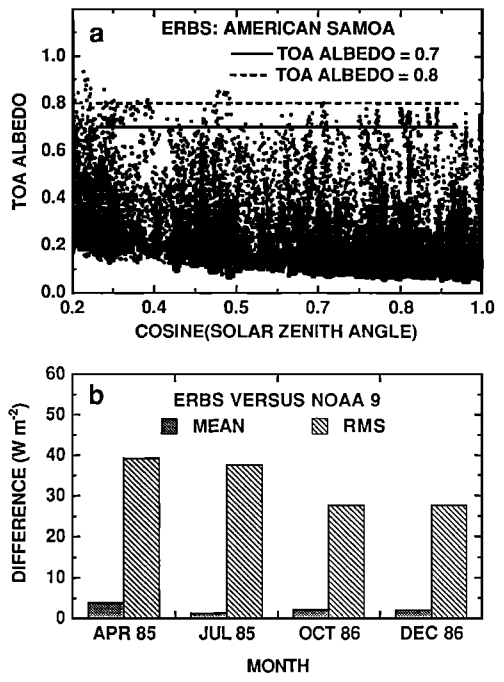

Figure 14. (a) Individual pixel measurements of the TOA albedo by the Earth Radiation Budget Satellite (ERBS) scanner for American Samoa, as a function of the cosine of the solar zenith angle. (b) Mean and RMS differences between temporally and spatially collocated ERBS and NOAA 9 pixel measurement of reflected SW radiation at the TOA.

Moreover, these differences are not an artifact of the narrowband GOES measurements, because the American Samoa and Cape Grim albedos were determined from measurements made by the Earth Radiation Budget Experiment (ERBE) broadband scanners.

In evaluating the maximum TOA albedo from the α-T scatterplots, it is important to recognize that averaging of individual pixel measurements has been performed, and it is useful to emphasize that individual pixel data should not be used to evaluate the maximum TOA albedo. To make this point, all of the ERBE TOA albedo pixel measurements that have gone into the collocated American Samoa data set are plotted in Figure 14a as a function of the cosine of the solar zenith angle. There are indeed individual pixel measurements that even exceed 0.8, but this is not inconsistent with the maximum observed TOA albedo for American Samoa shown in Figure 13b. Instead, the spiky behavior demonstrated by the data at the top of Figure 14a has always been attributed to the angular-directional models (ADMs) used to convert radiance to flux. This is consistent with scanner-to-scanner intercomparisons of reflected SW radiation at the TOA, which show large RMS differences but a small-mean difference. Such an example is shown in Figure 14b for 203,571 spatially and temporally collocated Earth Radiation Budget Satellite (ERBS) and NOAA 9 pixel pairs. The point is that the ADM error for individual pixels is reduced to a small difference when averaging is performed over a large number of pixels, and this is precisely what has been done in going from Figure 14a to the American Samoa maximum TOA albedo shown in Figure 13b.

An alternate approach is to use measurements that do not require the use of ADMs, such as the hemispherical instruments flown on the NASA ER-2 during the Central Equatorial

Pacific Experiment (CEPEX) and Tropical Ocean Global Atmosphere-Coupled Ocean Atmosphere Response Experiment (TOGA-COARE). These aircraft altitude albedos are shown in Figure 15, and they demonstrate a clearly defined upper boundary that is consistent with a TOA albedo of 0.7. The aircraft-altitude albedo differs from the TOA albedo because of absorption by stratospheric gases (mainly ozone), and we have used a radiation model to convert TOA albedos of 0.7 and 0.8 to aircraft altitude; these are depicted by the horizontal lines in Figure 15. These data are 3-min averages and represent a flight path of roughly 30 km, similar to the size of an ERBS pixel (35 km at nadir). For the CEPEX data, we also employed 1-min averaging and found the same maximum albedos as for 3-min averaging. The point is that the aircraft observations are totally consistent with the maximum TOA albedos shown in Figure 13b. We simply do not observe TOA albedos greater than 0.7, well below the value of 0.8 that models can produce.

4. Discussion of Related Studies

In addition to the investigations summarized in the Introduction, there have been two additional studies addressing the issue of cloud SW absorption. *Li et al.* [1995] claim that substantial excess cloud absorption occurs in the tropics, consistent with *Ramanathan et al.* [1995], *Cess et al.* [1995], and *Pilewskie and Valero* [1995] but not in the extratropics, which is inconsistent with *Cess et al.* [1995]. In the following paragraphs, we present some insights into their analyses.

Li et al. [1995] employed two procedures, one restricted to a site in Germany employing the $\Delta\alpha/\Delta T$ slope as in Figure 10b. We have reproduced their Figure 4 for Germany (our Figure 16a), as well as providing a similar analysis for a region in France (Figure 16b), using the same monthly-mean satellite and surface data as did Li et al. Also shown are slopes generated from CCM2 for the two regions, which show only modest departures from the observed slopes. To place these results in perspective, the Wisconsin data, as described in section 2, are included in Figure 16c. Comparison of these three extratropical regions underscores one aspect of the Li et al. [1995] and *Cess et al.* [1995] disagreement; the observed versus CCM2 slope differences are marginal for France and Germany, consistent with the Li et al. interpretation, whereas for Wisconsin they are substantial, consistent with our Boulder comparison shown in Figure 12.

The albedo transmittance dynamic range, however, is considerably smaller for Germany and France than for Wisconsin because *Li et al.* [1995] used monthly-mean data, whereas for Wisconsin we used near-instantaneous data spanning the range from clear skies on the right to heavily overcast conditions on the left (Figure 16c). To be a measure of cloud absorption, the slope must be due solely to cloudiness variations, and because of the reduced dynamic range of the monthly-mean data for Germany and France, it is possible that their slopes are being influenced by other factors. To test this possibility, we have evaluated $\Delta\alpha/\Delta T$ for CCM2 using (1) with annual-mean values for CRF(TOA)/CIF(SRF). These values are compared in Figure 17a to $\Delta\alpha/\Delta T$, as evaluated from a scatterplot of instantaneous α versus T output. As for the Boulder data (Figure 12), these two slope estimates are virtually identical. However, when monthly-mean output is used the slope magnitudes are greater, and this provides a plausible explanation as to why the slope magnitudes for Germany and France are greater than for Wisconsin (Figure 16); they are being influenced by factors other than cloudiness variability. When CCM2 is compared to the observations in a consistent manner, by using monthly-mean output from CCM2 rather than instantaneous output so as to be compatible with the monthly-mean data, the $\Delta\alpha/\Delta T$ differences shown in Figure 17b are substantially larger than those shown in Figures 16a and 16b. Thus it is doubtful that an α-T slope, generated from monthly-mean data as in Figure 4 of Li et al. [1995] provides information that can be used to appraise cloud SW absorption.

Li et al. [1995] also considered the ratio of cloud-radiative forcing at the surface to that at the TOA, as determined from global data in conjunction with two satellite retrieval algorithms that determine the clear-sky SW absorption at the sur-

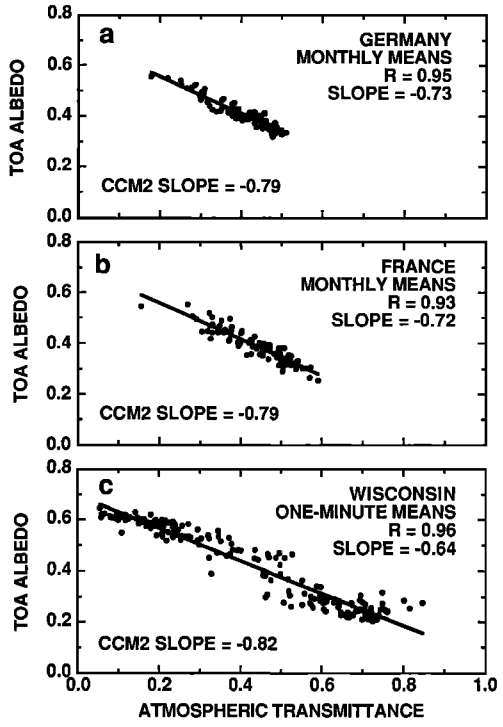

Figure 16. (a) The monthly mean data for TOA albedo as a function of the atmospheric transmittance for a region in Germany. (b) The same as Figure 16a but for a region in France. (c) The same as Figure 16a, but for near-instantaneous spatially averaged data for Wisconsin.

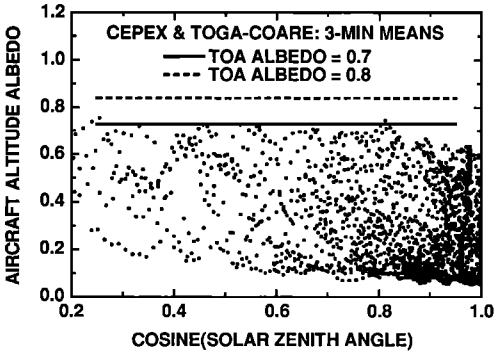

Figure 15. Aircraft altitude albedos measured from the NASA ER-2 during CEPEX and Tropical Ocean Global Atmosphere-Coupled Ocean Atmosphere Response Experiment, as a function of the cosine of the solar zenith angle.

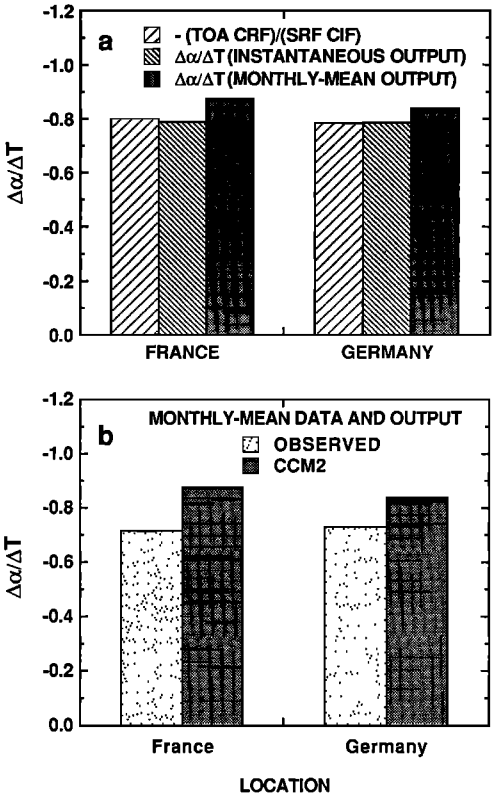

Figure 17. (a) Comparisons of $\Delta\alpha/\Delta T$ from CCM2 output using (1) with annual mean output, directly determined as the α-T slope using instantaneous output and directly determined from the α-T slope using monthly mean output. (b) Comparisons of $\Delta\alpha/\Delta T$ determined as the α-T slope using monthly-mean CCM2 output.

face, and the surface albedo. However, monthly-mean input was used in the first algorithm, as opposed to integrating over the diurnal cycle [*Li and Leighton*, 1993]. The surface albedo algorithm was used to convert surface insolation to surface absorption, and it is important to realize that since the albedo is the ratio of surface reflection to surface insolation, its monthly mean is determined as the ratio of mean quantities rather than by implementing monthly-mean input to an instantaneous algorithm, as was done [*Staylor and Wilber*, 1990] in the algorithm-derived surface albedos used by *Li et al.* [1995]. In addition, the monthly-mean cosine of the solar zenith angle was incorrectly evaluated by *Staylor and Wilber* [1990]. Given the inherent uncertainties associated with satellite retrieval algorithms, plus the implementation problems discussed above, it is doubtful the measurement-algorithm approach of *Li et al.* [1995] can either prove (tropics) or disprove (extratropics) the existence of excess cloud SW absorption.

The second study addressing cloud SW absorption is by *Imre et al.* [1996], who conclude that cloud SW absorption "is consistent with the traditional view of clouds"; that is, enhanced cloud SW absorption is insignificant. They used the same April 1994 ARM surface measurements as did T. Alberta and T. Charlock (private communication, 1996) (Figure 1), together with collocated GOES satellite measurements at the TOA. *Imre et al.* [1996] analyzed the data in much the same way as our present analyses of the collocated data at the BAO tower, and there are three potential problems with the data they used. First, as previously discussed, there is recent evidence that there may be a bias error in the surface measurements. Second, there has been a recent revision of the collocated GOES TOA measurements, so that the data they used is no longer current. Third, to evaluate the net SW absorption at the surface, they employed a downward facing instrument that viewed only a small portion of the satellite grid because it was mounted on a 10-m tower (in contrast to the 300-m tower at Boulder). However, recent measurements indicate that the surface albedo is highly variable over the ARM site and that the surface below the 10-m tower is not representative of the satellite grid.

Imre et al. [1996] acknowledge that there may be uncertainties associated with the GOES TOA measurements they used and claim that if this is the case then "all GOES based studies must be considered inconclusive." The point they have missed is that earlier GOES data, such as for the BAO tower and Wisconsin, employed ERBE data as a calibration reference, whereas ERBE data were not available for that purpose in April 1994.

5. Discussion of Results

Current views on the issue of cloud SW absorption tend to fall in the following three categories: those who believe that enhanced cloud SW absorption exists; those who believe that enhanced atmospheric absorption exists but that it is related to deficiencies in our understanding of clear-sky absorption rather than cloud absorption; and those who feel the models are essentially robust. The present results, combined with the studies by *Ramanathan et al.* [1995], *Cess et al.* [1995], *Pilewskie and Valero* [1995], and *Waliser et al.* [1996], collectively make a rather compelling case that models underestimate atmospheric SW absorption by underestimating cloud absorption. None of these studies have found that clear skies are the source of the problem. The present study has demonstrated that CCM2 is in excellent agreement with clear-sky atmospheric absorption measured at the BAO tower (Figure 3), while the agreement of CCM2 with the Wisconsin data for large transmittances representative of clear skies (Figure 13a) makes the same point. A recent analysis of CEPEX data for the tropical western Pacific (W. C. Conant, et al., An examination of the clear-sky solar absorption over the central equatorial Pacific: Observations versus models, submitted to *Journal of Climate*, 1996) concludes that "radiation models agree to within 4 W m^{-2} of the observed average clear-sky ocean and atmospheric solar heating." It should be noted that model simulated clear-sky transmittance and absorptance may differ from observations at locations where large concentrations of atmospheric aerosols exist. In such cases the detection of cloud absorption would become more difficult. However, this is not the case for the data used in this study.

To be more explicit on this point, we have extended the clear-sky comparison of CCM2 with the collocated data at the BAO tower to include SW absorption by the surface-atmosphere system (net downward SW at the TOA), by the surface, and by the atmosphere. As demonstrated in Figure 18a, the clear-sky agreement is quite remarkable. The inclusion of clouds considerably alters the situation, however, as shown by the all-sky comparison in Figure 18b. Note that CCM2 overestimates the net downward SW flux at the TOA by 32 W m^{-2}, meaning that it underestimates reflection at the TOA by the same amount. This is not, however, inconsistent with the suggestion that model clouds are brighter than real clouds. In Figure 18b this effect has been countered by CCM2 underes-

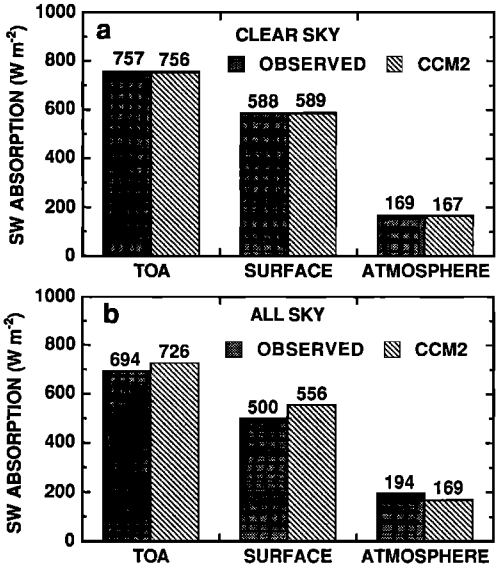

Figure 18. Comparisons between observations and CCM2 for the BAO tower, (a) for clear-sky conditions and (b) for all-sky conditions, for the SW absorption by the surface-atmosphere system (net downward SW at the TOA), by the surface, and by the atmosphere.

timating cloud optical depth, as was discussed with reference to Figure 11a. This underestimate is consistent with CCM2 producing a TOA CRF of only -30 W m^{-2}, compared to -63 W m^{-2} from the observations. A part of the 56 W m^{-2} overestimate in surface absorption by CCM2 is likewise attributed to its underestimate of cloud optical depth.

The meaningful comparisons are those for atmospheric absorption, which is the difference between the TOA and surface absorption. As in Figure 3b, atmospheric absorption by CCM2 is virtually invariant to the presence of clouds (Figure 18b versus Figure 18a). This is consistent with the interpretation by *Ramanathan et al.* [1995] that observed excess all-sky SW absorption relative to clear skies (Figure 2) in turn represents excess cloud absorption relative to models because models produce the same all-sky and clear-sky absorption as we have demonstrated for CCM2. The observed all-sky absorption is 25 W m^{-2} greater than for CCM2 and represents a dayside mean. The corresponding diurnal mean is 15 W m^{-2}, consistent with the 16 W m^{-2} of Figure 3a, which was determined from the difference between TOA and surface CRFs as in the work by *Ramanathan et al.* [1995].

We have previously suggested that model clouds are brighter and also transmit more SW radiation to the surface than do real clouds, with both effects being attributed to model clouds absorbing less SW radiation than do real clouds. These suggestions need to be clarified with respect to the method of interpretation that is used. The interpretation given in Figures 2 and 3a implicitly assumes the model is constrained to the same TOA CRF as observed, and this interpretation is illustrated in Figure 19 for the data at the BAO tower. To be consistent with Figure 18, dayside means have been adopted in Figure 19 rather than the diurnal means in Figure 3a. Because a model produces nearly the same CRF at the surface as at the TOA, then when constrained to the observed TOA CRF it would produce a surface CRF of -63 W m^{-2}, larger by 25 W m^{-2} than observed. Thus in this interpretation, the real clouds produce greater cooling at the surface because they allow 25 W m^{-2} less SW radiation to reach the surface as a consequence of absorbing 25 W m^{-2} more SW radiation than do the model clouds. Thus, when a model is constrained to the TOA observations, the interpretation of enhanced cloud SW absorption is that it reduces the surface insolation and in turn the atmospheric transmittance.

When interpreting real clouds as being darker than model clouds, the implicit interpretation in this study is that the model is being constrained to the surface insolation measurements, and thus the observed atmospheric transmittance, as demonstrated in Figure 13a for the Wisconsin data. This constraint vanishes, however, in the limit of thick clouds ($T \rightarrow 0$), which addresses the issue of the maximum possible TOA albedo.

On the other hand, the comparison shown in Figure 18 imposes no constraint at all, with the TOA and surface all-sky differences being a combination of differences in cloud absorption and cloud optical depth. However, the latter does not impact the model's all-sky atmospheric absorption, as previously discussed, and thus the 25 W m^{-2} difference in all-sky atmospheric absorption is attributable solely to cloud absorption, as is consistent with Figure 19. The point is that the implied cloud absorption is invariant as to whether the model is constrained to either the TOA or the surface measurements or is unconstrained.

Our suggestion that real clouds produce maximum TOA albedos that are lower than those for models, as demonstrated in Figures 14a and 15, is likewise independent as to how a model is constrained. Moreover, this conclusion is consistent with *Stephens and Greenwald* [1991, p. 15, 337], who concluded "the observed albedo of clouds are significantly lower than the modeled albedos assuming plane-parallel radiative transfer theory and realistic microphysics." Neither Stephens and Greenwald nor the present study address the issue of ice or mixed-phase clouds; CCM2 generates only liquid water clouds. However, if the presence of ice clouds were to eliminate, at least regionally, observational-model differences in the maximum TOA albedo, they should likewise eliminate the observational-model differences in cloud SW absorption. *Lubin et al.* [1996] have shown that this is not the case.

6. Concluding Remarks

Our examination of spatial and temporal sampling errors has provided a better understanding as to the interpretation of collocated satellite and surface SW measurements. Further-

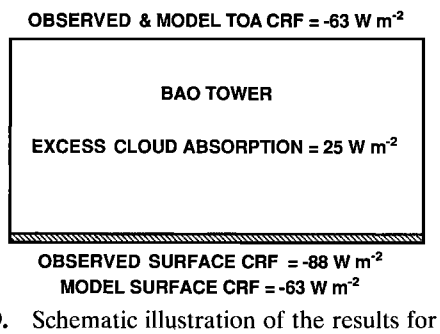

Figure 19. Schematic illustration of the results for the BAO tower when a model is constrained to the observed TOA CRF. These quantities represent dayside means, whereas Figure 3a refers to diurnal means.

more, we have demonstrated several ways of isolating cloud SW absorption, all of which consistently show that clouds absorb more SW radiation than predicted by theoretical models.

Neither this study nor any of the others that indicate the existence of enhanced cloud SW absorption provide any explanation as to the cause of the phenomenon. As discussed in the Introduction, cloud morphology constitutes one possible candidate for increasing cloud SW absorption relative to conventional plane-parallel cloud models. Another possible mechanism refers to our potential lack of understanding of SW absorption by atmospheric water vapor. In an experimental study of the transmission of near-infrared radiation (1.3–2.5 μm) through water vapor, *Goldstein and Penner* [1964, p. 359] state that "it is interesting to note the rather abrupt change in transmission just before saturation conditions are reached." The abrupt change they refer to denotes an increase in absorption as saturation is approached. If such a phenomenon occurs for atmospheric water vapor, it would primarily manifest itself within clouds rather than in the clear atmosphere, because it is within clouds that water vapor approaches saturation and can even become supersaturated.

Acknowledgments. We are grateful to Gary G. Gibson for providing us with the ERBS and NOAA 9 scanner intercomparison statistics that are summarized in Figure 14b, to Peter Pilewskie for the ER-2 TOGA-COARE albedos shown in Figure 15, and to Bruce P. Briegleb for performing the CCM2 simulation. This work was supported by the Department of Energy through grant DEFG0285ER60314 and DEFG0290ER61063 and by the National Aeronautics and Space Administration through grant NAG11264 and NAGW3517.

References

Ackerman, S. A., and S. K. Cox, Aircraft observations of shortwave fractional absorptance of non-homogeneous clouds, *J. Appl. Meteorol.*, *20*, 1510–1515, 1981.

Byrne, R. N., R. C. J. Somerville, and B. Subasilar, Broken-cloud enhancement of solar radiation absorption, *J. Atmos. Sci.*, *53*, 878–886, 1996.

Cess, R. D., et al., Absorption of solar radiation by clouds: Observations versus models, *Science*, *267*, 496–499, 1995.

Chou, M. D., A. Arking, J. Otterman, and W. L. Ridgway, The effect of clouds on atmospheric absorption of solar radiation, *Geophys. Res. Lett.*, *22*, 1885–1888, 1995.

Fritz, S., Solar radiant energy, in *Compendium of Meteorology*, edited by T. F. Malone, pp. 14–29, John Wiley, New York, 1951.

Fu, Q., and K.-N. Liou, Parameterization of the radiative properties of cirrus clouds, *J. Atmos. Sci.*, *50*, 2008–2025, 1993.

Goldstein, R., and S. S. Penner, Transmission of infrared radiation through liquid water and through water vapor near saturation, *J. Quant. Spectrosc. Radiat. Transfer*, *4*, 359–361, 1964.

Imre, D. G., E. H. Abramson, and P. H. Daum, Quantifying cloud-induced shortwave absorption: An examination of uncertainties and of recent arguments for large excess absorption, *J. Appl. Meteorol.*, in press, 1996.

Kiehl, J. T., J. J. Hack, M. H. Zhang, and R. D. Cess, Sensitivity of a GCM climate to enhanced shortwave cloud absorption, *J. Clim.*, *8*, 2200–2212, 1995.

King, M. D., L. F. Radke, and P. V. Hobbs, Determination of the spectral absorption of solar radiation by marine stratocumulus clouds from airborne measurements within clouds, *J. Atmos. Sci.*, *47*, 894–907, 1990.

Li, Z., and H. G. Leighton, Global climatology of solar radiation budgets at the surface and in the atmosphere from 5 years of ERBE data, *J. Geophys. Res.*, *98*, 4919–4930, 1993.

Li, Z., H. W. Barker, and L. Moreau, The variable effect of clouds on atmospheric absorption of solar radiation, *Nature*, *376*, 486–490, 1995.

Liou, K.-N., *Radiation and Cloud Processes in the Atmosphere: Theory, Observation and Modeling*, Oxford Univ. Press, New York, 1992.

Loeb, N. G., and R. Davies, Observational evidence of plane parallel model biases: Apparent dependence of cloud optical depth on solar zenith angle, *J. Geophys. Res.*, *101*, 1621–1634, 1996.

Long, C. N., and T. P. Ackerman, Surface measurements of solar irradiance: A study of the spatial correlation between simultaneous measurements at separated sites, *J. Appl. Meteorol.*, *34*, 1039–1046, 1995.

Lubin, D., J. P. Chen, P. Pilewskie, V. Ramanathan, and F. P. J. Valero, Microphysical examination of excess cloud absorption in the tropical atmosphere, *J. Geophys. Res.*, *101*, 16,961–16,972, 1996.

Minnis, P., P. W. Heck, D. F. Young, C. W. Fairall, and J. B. Snider, Stratocumulus cloud properties derived from simultaneous satellite and island-based instrumentation during FIRE, *J. Appl. Meteorol.*, *31*, 317–339, 1992.

Minnis, P., P. W. Heck, and D. F. Young, Inference of cirrus cloud properties using satellite-observed visible and infrared radiances, II, Verification of theoretical cirrus radiative properties, *J. Atmos. Sci.*, *50*, 1305–1322, 1993.

Pilewskie, P., and F. P. J. Valero, Direct observations of excess solar absorption by clouds, *Science*, *267*, 1626–1629, 1995.

Pilewskie, P., and F. P. J. Valero, Response to "How much solar radiation do clouds absorb?," *Science*, *271*, 1134–1136, 1996.

Ramanathan, V., et al., Warm pool heat budget and shortwave cloud forcing: A missing physics?, *Science*, *267*, 499–503, 1995.

Staylor, W. F., and A. C. Wilber, Global surface albedo estimated from ERBE data, paper presented at 7th Conference on Atmospheric Radiation, Am. Meteorol. Soc., Boston, Mass., 1990.

Stephens, G. L., and T. J. Greenwald, The Earth's radiation budget and its relation to atmospheric hydrology, 2, Observations of cloud effects, *J. Geophys. Res.*, *96*, 15,325–15,340, 1991.

Stephens, G. L., and S.-C. Tsay, On the cloud absorption anomaly, *Q. J. R. Meteorol. Soc.*, *116*, 671–704, 1990.

Waliser, D. E., W. D. Collins, and S. P. Anderson, An estimate of the surface shortwave cloud forcing over the western Pacific during TOGA COARE, *Geophys. Res. Lett.*, *23*, 519–522, 1996.

Wild, M., A. Ohmura, H. Gilgen, and E. Roeckner, Validation of general circulation model radiative fluxes using surface observations, *J. Clim.*, *8*, 1309–1324, 1995.

R. D. Cess, V. Dvortsov, X. Jing, M. H. Zhang, and Y. Zhou, Institute for Terrestrial and Planetary Atmospheres, Marine Sciences Research Center, State University of New York, Stony Brook, NY 11794-5000.

(Received February 13, 1996; revised June 5, 1996; accepted June 5, 1996.)